Published in final edited form as:
Nat Neurosci. 2005 July ; 8(7): 881–888. doi:10.1038/nn1478.

Nonclassical, distinct endocytic signals dictate constitutive and PKC-regulated neurotransmitter transporter internalization

Katherine L Holton[1], **Merewyn K Loder**[1], and **Haley E Melikian**[1,2,3]

1*Brudnick Neuropsychiatric Research Institute, Department of Psychiatry, University of Massachusetts Medical School, 303 Belmont Street, Worcester, Massachusetts 01604, USA*

2*Program in Neuroscience, University of Massachusetts Medical School, 303 Belmont Street, Worcester, Massachusetts 01604, USA*

3*Department of Biochemistry and Molecular Pharmacology, University of Massachusetts Medical School, 303 Belmont Street, Worcester, Massachusetts 01604, USA*

Abstract

Neurotransmitter transporters are critical for synaptic neurotransmitter inactivation. Transporter inhibitors markedly increase the duration and magnitude of synaptic transmission, underscoring the importance of transporter activity in neurotransmission. Recent studies indicate that membrane trafficking dynamically governs neuronal transporter cell-surface presentation in a protein kinase C-regulated manner, suggesting that transporter trafficking profoundly affects synaptic signaling. However, the molecular architecture coupling neurotransmitter transporters to the endocytic machinery is not defined. Here, we identify nonclassical, distinct endocytic signals in the dopamine transporter (DAT) that are necessary and sufficient to drive constitutive and protein kinase C-regulated DAT internalization. The DAT internalization signal is conserved across SLC6 neurotransmitter carriers and is functional in the homologous norepinephrine transporter, suggesting that this region is likely to be the endocytic signal for all SLC6 neurotransmitter transporters. The DAT endocytic signal does not conform to classic internalization motifs, suggesting that SLC6 neurotransmitter transporters may have evolved unique endocytic mechanisms.

Neuronal plasma membrane transporters mediate high-affinity neuro-transmitter reuptake, the primary mechanism limiting extracellular neurotransmitter levels and terminating synaptic transmission. The dopamine (DA) transporter belongs to the high-affinity, Na^+/Cl^--dependent SLC6 transporter gene family, which also includes norepi-nephrine (NE), serotonin (5-HT), GABA and glycine neurotransmitter transporters[1,2]. DAT is a major psychostimulant target in the brain, and cocaine, amphetamine and methylenedioxymethamphetamine ('ecstasy') inhibit DA reuptake by competing for the DA binding site[3,4]. Pharmacological[5,6] and genetic[7,8] DAT suppression markedly extends extracellular DA half-life and enhances postsynaptic responses, underscoring the central role that DAT activity plays in normal dopaminergic transmission. Moreover, DA tissue stores are significantly depleted in both *DAT*$^{+/-}$(also known as *Sl6ca3*$^{+/-}$) and *DAT*$^{-/-}$ mice[7], indicating that transporter-facilitated DA recapture is essential for maintaining normal dopaminergic tone. Taken together, these results indicate that DAT activity markedly affects DA synaptic transmission, transmitter homeostasis and psychostimulant targeting.

Correspondence should be addressed to H.E.M. (haley.melikian@umassmed.edu)..

COMPETING INTERESTS STATEMENT
The authors declare that they have no competing financial interests.

Considering its central role in shaping dopaminergic signaling, DAT is a likely target for cellular regulation. Indeed, copious evidence demonstrates that protein kinase C (PKC) acutely downregulates DAT[2,9-11] by rapidly sequestering DAT from the plasma membrane to intracellular endosomes in a membrane trafficking-dependent manner[12,13]. DAT trafficking is not limited to regulatory events, as recent studies have shown dynamic basal DAT cycling between the cell surface and intracellular endosomal compartments at endocytic rates that can reach 3-5% per minute[14,15], with similar evidence also reported for constitutive GABA transporter (GAT) movement in hippocampal neurons[16,17]. PKC-stimulated DAT sequestration is achieved by simultaneously increasing basal DAT endocytic rates and slowing DAT cell-surface delivery[9,15]. Similar kinetic changes in transporter movement acutely modulate both GABA and 5-HT transporters in response to substrates[17,18], protein kinase G[19] and tyrosine kinase activity[17,20,21]. Given the fundamental role of membrane trafficking in neurotransmitter transporter regulation, a greater understanding of the molecular determinants governing transporter trafficking is likely to shed light on these pivotal synaptic regulators.

A requisite step for protein internalization is interaction with the cellular endocytic machinery. For clathrin-mediated endocytosis, adaptor proteins link putative cargo proteins to clathrin, thereby directing them into clathrin-coated pits[22,23]. Although SLC6 neurotransmitter transporters robustly internalize, the endocytic signals targeting neurotransmitter transporters for constitutive and regulated internalization are virtually unknown. In the present study, we sought to define the endocytic signal(s) driving basal and PKC-regulated DAT internalization. Our results demonstrate that distinct, but overlapping, endocytic motifs in the DAT C terminus independently mediate constitutive and PKC-regulated DAT endocytosis. The DAT endocytic signal is highly conserved across the SLC6 gene family, and the orthologous domain is critical for norepinephrine transporter (NET) internalization, suggesting that this sequence is likely to be necessary for endocytosis of multiple SLC6 neurotransmitter transporters and therefore may be a key regulatory target in controlling neurotransmitter transporter surface levels.

RESULTS

DAT carboxyl tail contains an autonomous endocytic signal

We sought to define the endocytic signal(s) necessary for constitutive and PKC-regulated DAT internalization. The DATamino acid sequence contains several candidate dileucine-type endocytic motifs at positions 10 (Leu-Met), 14 (Val-Val), 31 (Leu-Ile-Leu-Val), 583 (Leu-Pro) and 603 (Leu-Val). We performed alanine-scanning mutagenesis at each of these loci and tested the constitutive and PKC-regulated endocytic capacity of these DAT mutants in transiently transfected PC12 cells. None of these potential endocytic signals was necessary for either constitutive or PKC-stimulated DAT internalization after 30 min of PMA treatment, as determined by DA uptake and cell-surface biotinylation (data not shown), suggesting that the DAT endocytic signal may not conform to classically defined motifs.

As a mutagenic (loss-of-function) approach was not successful in defining DAT endocytic signal(s), we turned to a gain-of-function approach to test whether specific DAT domains encoded information sufficient to rescue internalization of endocytic-defective reporter molecules. To this end, we fused the DAT N and C termini to the Δ3-59 transferrin receptor (TfR; Fig. 1a) and interleukin 2α receptor (Tac, Fig. 2a), respectively, and assessed their endocytic abilities. These proteins are readily expressed at the plasma membrane but are unable to constitutively internalize; however, appending them with viable endocytic motifs can rescue their endocytic potential[24-27]. Single-cell internalization assays showed that although the DAT1-44/TfRΔ3-59 chimera was expressed and transported to the cell surface, it did not internalize as wild-type TfR did (Fig. 1), suggesting that the DAT N terminus does not contain an autonomous endocytic signal. Tac targeted the plasma membrane and was endocytic-

defective, as previously reported[26,27] (Fig. 2b and Table 1). In contrast, a Tac-DAT chimera in which DAT C-terminal residues 582-620 were fused to Tac robustly internalized (Fig. 2b and Table 1), suggesting that a constitutive endocytic signal is contained in the DAT C terminus.

To narrow the region containing the putative DAT endocytic signal, we truncated the DAT C terminus within the Tac-DAT context and evaluated whether the resulting chimeras could internalize (Fig. 2b and Table 1). To rule out any contribution by DAT's C-terminal PDZ binding domain[28-30], all truncation mutants retained the carboxyl WLKV sequence (residues 617-620). Eliminating DAT residues 597-616 had no effect on Tac-DAT internalization (Fig. 2b and Table 1), suggesting that the 587-596 region alone was sufficient to drive Tac endocytosis. Deleting only the 587-596 stretch abolishedTac-DAT internalization (Fig. 2b and Table 1), indicating that this subdomain is absolutely required for Tac-DAT endocytosis and is a strong candidate for the DAT endocytic signal.

DAT residues 587-596 correspond to the amino acid sequence FREKLAYAIA, which does not conform to any previously defined endocytic signal. To further delineate the DAT endocytic signal within the FREKLAYAIA sequence, we mutated single and multiple DAT residues to alanines in the Tac-DAT chimera and assessed their endocytic ability (Fig. 3a and Table 1). Tac-DAT internalization was abolished when either all ten or the five carboxy-most residues within the FREKLAYAIA DAT subsequence were mutagenized (Tac-DAT 587-596(10A) and Tac-DAT 592-596(5A), respectively). Mutagenizing the five upstream residues (Tac-DAT 587-591(5A)) did not significantly reduce Tac-DAT internalization (Fig. 3b and Table 1), although there was a trend toward loss of Tac-DAT internalization, suggesting that the FREKL residues may contain valid DAT endocytic information. Further mutagenesis of single nonpolar residues within the LAYAIA sequence (Fig. 3c) revealed that Tac-DAT internalization was completely dependent on Ile595 but did not require Leu591 or Tyr593 (Fig. 3d and Table 1), suggesting that Ile595 is a critical determinant within the DAT endocytic signal. Loss of Tac-DAT I595A endocytosis was not due to globally diminished endocytosis, as transferrin uptake was unaffected by Tac-DATI595A expression (Fig. 3d), indicating that the Tac-DAT I595A mutation specifically perturbs the DAT endocytic signal.

Although the FREKLAYAIA domain is sufficient to drive Tac internalization, it may not be required for full-length DAT internalization. To test this possibility, we independently converted DAT residues Leu591, Tyr593 and Ile595 to alanines in full-length DATand measured the relative endocytic rates of the resulting DATmutants L591A, Y593A and I595A. DAT point mutants L591A, Y593A and I595A expressed steady-state distributions similar to that of wild-type DAT as determined by steady-state biotinylation (data not shown). It should be noted, however, that a disproportionate amount of 58-kDa DAT I595A was detected by immunoblot (data not shown), consistent with the immature (endoplasmic reticular) form of DAT[13,14] and suggesting that this mutant may not exit the endoplasmic reticulum comparably to wild-type DAT. Using a biotinylation-based internalization assay, we measured wild-type DAT endocytosis at rates of 3-5% per minute (Fig. 4), consistent with previous results from our group[15] and others[14]. Notably, mutating any of the nonpolar residues within the LAYAIA stretch significantly reduced DAT endocytic rates to levels consistent with bulk membrane turnover (~1% per minute, $P < 0.01$, Fig. 4). In contrast, mutating either upstream (LP583AA) or downstream (LV603AA) nonpolar residues did not significantly affect constitutive DAT internalization (Fig. 4b), consistent with the premise that the LAYAIA region is specifically required for DAT endocytosis.

DAT endocytic signal is conserved within SLC6 gene family

The FREKLAYAIA region is well conserved among mammalian SLC6 neurotransmitter transporters (Fig. 5a), raising the possibility that it may serve as the endocytic signal for these

carriers. We tested this hypothesis by asking whether the cognate NET C-terminal region could drive Tac endocytosis. Indeed, NET C-terminal residues 580-617 were sufficient to stimulate Tac-NET chimera endocytosis (Fig. 5b), consistent with the hypothesis that the NET C-terminal domain containsan endocytic signal. To test whether the cognate FREKLAYAIA region was also required for NET internalization, we compared the endocytic capacity of full-length wild type NET to a mutant NET in which all ten amino acids were converted to alanines (NET584-593(10A)). Similar to our results with DAT, wild-type NET showed robust constitutive internalization of approximately 3% per minute (Fig. 5c). In contrast, NET584-593 (10A) was significantly impaired in its ability to internalize (Fig. 5c), consistent with the notion that this region contains the NETendocytic signal and suggesting that the FREKLAYAIA subdomain is likely to contain critical endocytic information for mammalian SLC6 neurotransmitter transporters.

DAT basal and PKC-sensitive endocytic signals are distinct

Given that endocytosis is essential for PKC-mediated DAT down-regulation and sequestration, we asked whether the nonpolar residues necessary for constitutive DAT internalization were also required for PKC-stimulated DAT sequestration. Notably, although they are unable to constitutively endocytose, the DAT mutants L591A, Y593A and I595A were functionally downregulated (Fig. 6a) and internalized (Fig. 6b), comparable to wild-type DAT, in response to acute PKC activation. These results suggest that independent endocytic signals may govern constitutive versus PKC-regulated DAT internalization.

Although PKC-stimulated DAT internalization did not require the FREKLAYAIA nonpolar residues, the C terminus may still contribute to PKC-regulated DAT endocytosis. To test this hypothesis, we used our Tac-DAT chimeras to ask whether PKC stimulation could drive endocytosis of the Tac-DAT I595A mutant, a chimera defective in constitutive internalization. Consistent with our earlier results, neither Tac nor Tac-DATI595A constitutively internalized (Fig. 7). However, PKC activation stimulated robust Tac-DAT I595A, but not Tac, endocytosis (Fig. 7a), suggesting that the DAT C terminus contains a PKC-regulated endocytic signal independent of Ile595. PKC-induced Tac-DAT internalization was observed when DAT amino acids 592-596 were alanine mutated (Tac-DAT 592-596(5A); Fig. 7a), but it was completely abolished when the entire FREKLAYAIA sequence was mutated (Tac-DAT 587-596(10A), Fig. 7a), suggesting that critical PKC-sensitive endocytic information might reside in DAT residues 587-591. We tested this possibility in full-length DAT by mutating either the entire FREKLAYAIA region (DAT587-596(10A)) or the FREKL sequence (DAT587-591(5A)) to alanines and assessing whether these mutants were capable of acute PKC-induced downregulation. Alanine substitution of either FREK-LAYAIA or FREKL completely abolished PMA-induced DAT downregulation, compared with wild-type DAT (Fig. 7b), suggesting that the FREKL sequence (DAT 587-591) is critical for PKC-mediated DAT downregulation.

Finally, we investigated whether the FREKLAYAIA sequence was an endocytic signal in the context of dopaminergic neurons by testing whether Tac, Tac-DAT or Tac-DAT 587-596(10A) could internalize when expressed in either immortalized mesencephalic neurons or primary ventral midbrain neurons. As in PC12 cells, the cell-surface marker Tac targeted the plasma membrane but did not internalize (Fig. 8). The DAT C terminus was sufficient to drive Tac internalization, both in immortalized mesencephalic neurons (Fig. 8a) and primary ventral midbrain neurons (Fig. 8b). Consistent with our results in PC12 cells, Tac-DAT endocytosis was completely dependent upon the FREKLAYAIA sequence in both cellular contexts (Fig. 8). Taken together, these results suggest that the FREKLAYAIA subdomain is the DAT endocytic signal and that it functions as such in a dopaminergic context.

DISCUSSION

Despite numerous reports describing constitutive and regulated transporter trafficking, the molecular mechanisms governing transporter endocytosis are not well defined. Here, we sought to define the endocytic signal(s) governing constitutive and PKC-regulated DAT internalization. Our results reveal a previously unknown C-terminal sequence that is both necessary and sufficient to drive DAT and NET endocytosis, suggesting that this signal is a likely endocytic determinant for mammalian neurotransmitter transporters within the SLC6 transporter family.

Most endocytic signals are highly conserved across divergent membrane protein classes and fall into two major categories: tyrosine- and dileucine-based[22]. Tyrosine-based motifs can be either NPXY, or YXXφ, where X can be any amino acid and φ is a large, bulky hydrophobic residue. Dileucine-based motifs are less strictly defined, but they typically contain a leucine followed by another nonpolar residue, with upstream acidic amino acids usually positioned -4 to -5 relative to the first leucine. DAT encodes a YXXφ-type tyrosine motif at Tyr335, but mutagenesis studies have recently ruled out any potential contribution of this residue to PKC-mediated DAT sequestration[31]. Clustal sequence analysis of mammalian SLC6 neurotransmitter transporters (rodent and primate) indicates a conserved sequence across the DAT FREKLAYAIA of L(X)ERLAY(X)IT. Notably, there is absolute conservation of a downstream flanking proline residue (Fig. 5a) suggestive of a secondary structure within this domain. Although well-conserved across mammalian neurotransmitter transporter members of the SLC6 gene family, the L(X)ERLAY(X)IT sequence does not conform to either classic dileucine- or tyrosine-based motifs. To determine whether this subsequence was recapitulated in other membrane proteins, or if it was unique to SLC6 transporters, we used a Hidden Markov Model to derive a transporter consensus sequence within the L(X)ERLAY(X)IT region and used this to search the non-redundant protein database. The results showed that the this subsequence is not reiterated in any other proteins but is highly conserved within mammalian SLC6 gene family members, suggesting that this region may serve as a novel endocytic signal solely for SLC6 neurotransmitter transporters.

The nature of the DAT endocytic signal raises the possibility that DAT endocytosis may be mediated by a clathrin-independent mechanism or that novel adaptor proteins may target DAT for internalization. Several lines of evidence suggest that PKC-mediated DAT internalization is clathrin-dependent, as the K44A dynamin mutant blocks both PKC[12]- and amphetamine-mediated[32] DATsequestration, and conconavalin A treatment blocks MAP kinase-dependent DAT trafficking[33]. However, since dynamin is required for a number of clathrin-independent forms of endocytosis, the possibility cannot be ruled out that a clathrin-independent mechanism governs DAT endocytosis. Consistent with this premise, a role for lipid rafts in PKC-stimulated NET internalization in primary trophoblasts has recently been reported[34].

Notably, constitutive DAT endocytosis was abrogated when any nonpolar residue within the FREKLAYAIA region was mutated (Fig. 4b), whereas the Tac-DAT chimera tolerated L591A and Y593A mutagenesis, but not I595A (Fig. 3d). The increased sensitivity of DAT over Tac-DAT may indicate that a higher-order structure within full-length DAT participates in the interaction of DAT with the endocytic machinery and that this structure is highly sensitive to the local environment within the FREKLAYAIA subdomain. Recent C-terminal truncation analysis of GAT demonstrated that the analogous Leu591 residue was essential for endoplasmic reticulum export, surface expression and Sec24 binding[35]. In our studies, the DAT L591A mutant was expressed and targeted to the plasma membrane, possibly indicating divergence in endoplasmic reticulum export criteria between GAT and DAT; or, it may reflect the different approaches used in the two studies (point mutagenesis versus truncation). Although we did not detect any anomalous plasma membrane expression of the L591A mutant

(data not shown), we did note a disproportionate amount of immature DAT I595A, suggesting that Ile595 may contribute to DAT maturation, endoplasmic reticulum exit or both. Furthermore, DAT mutants L591A and Y593A showed steady-state distributions similar to those of wild-type DAT, despite lacking constitutive internalization (data not shown). These findings suggest that DAT recycling rates may also be affected by FREKLAYAIA mutations or that other cellular compensatory mechanisms may exist to maintain minimal DAT surface levels under basal conditions.

We asked whether residues critical for constitutive DAT trafficking were also necessary for PKC-regulated DAT internalization and sequestration. Point mutations disrupting basal DAT endocytosis had no effect on PKC-stimulated DAT internalization (Fig. 6), suggesting that independent mechanisms mediate constitutive and PKC-stimulated transporter internalization. This agrees with our previous observation that constitutive and PKC-stimulated DATendocytosis are differentially saturable[15], consistent with the notion that distinct cellular mechanisms govern these two processes.

Although residues Leu591, Y593 and Ile595 were not necessary for PKC-stimulated DAT sequestration, studies with the Tac-DAT reporter molecule and mutagenesis of full-length DAT demonstrated that the FREKLAYAIA stretch was required for PKC-induced DATsequestration (Fig. 7a). Moreover, PKC-mediated DAT downregulation was absolutely dependent upon the FREKL residues, further supporting the hypothesis that constitutive and regulated DAT internalization may be mechanistically distinct. The close opposition of the constitutive and PKC-regulated DATendocytic signals is intriguing, and it is tempting to speculate that these two signals may operate synergistically to orchestrate basal and regulated DAT internalization. The upstream conservation of a potential serine/threonine phosphoacceptor site (Fig. 5a) raises the possibility that PKC-induced DAT phosphorylation may either interact with or be targeted to this domain. A more in-depth exploration of the relationship between constitutive and PKC-regulated DATendocytosis is beyond the scope of this study, but future investigations should shed light on this possibility.

A variety of neuronal regulatory events rely on membrane trafficking, including growth factor signaling[36,37] and synaptic plasticity[38,39]. Given that transmitter reuptake is critical for temporospatially constraining synaptic transmission, trafficking-mediated transporter regulation is optimally suited to contribute to synaptic efficacy and plasticity. A number of cellular signaling pathways regulate transporter trafficking[2,9-11], suggesting that multiple inputs can be integrated to dynamically shape the profile of transporter surface presentation. Indeed, a recent study demonstrates a reciprocal relationship between tyrosine kinase- and PKC-mediated GAT1 trafficking[21], indicating that such signal integration is likely to exist. Our results defining transporter endocytic determinants provide an initial step in understanding the molecular requirements underlying transporter movement in neurons and are likely to ultimately shed light on transporter contributions to synaptic plasticity.

METHODS

Materials

Phorbol 12-myristate 13-acetate (PMA) and holo-transferrin were from Calbiochem and GBR12909 was from Tocris-Cookson. Rat anti-DAT, rabbit anti-tyrosine hydroxylase and all horseradish peroxidase-conjugated secondary antibodies were from Chemicon. Fluorescently labeled secondary antibodies and transferrin were from Molecular Probes. All cell culture reagents were from Invitrogen unless otherwise noted. All other reagents were purchased from Sigma-Aldrich unless otherwise noted.

cDNA constructs

hTac pcDM8.1 and hTfR pCMV plasmids were donated by J. Bonafacino (US National Institutes of Health, Bethesda, Maryland) and T.E. McGraw (Weill College of Medicine, Cornell University, New York), respectively, and hDAT pcDNA3.1(+) was derived as previously described[13]. The cDNA encoding the hNET was the gift of R. Blakely (Vanderbilt University, Nashville, Tennessee) and was subcloned into pcDNA 3.1(+) at the *Xho*I/*Xba*I sites. Coding regions for TfR and Tac were excised and subcloned into pcDNA 3.1(+) (Invitrogen) at the *Bam*HI/*Xho*I and *Sal*I/*Xba*I sites, respectively. All truncations were generated using PCR to insert double stop codons at the desired position. Chimeric reporter-DAT proteins were generated using the PCR-ligation-PCR method[40], and mutagenesis was performed with the Quick-Change mutagenesis kit (Stratagene). All Tac and hDAT mutated regions were excised and re-ligated back into their parental plasmids at the *Bsu*36I/*Xba*I and *Cla*I/*Xba*I sites, respectively. All sequences were confirmed by the University of Massachusetts Medical School Nucleic Acid Facility.

Cell culture and transfections

PC12 cells were maintained as previously described[13] and were plated on poly-D-lysine-coated 24-well or 6-well plates at densities of 2.1×10^5/well and 1×10^6/well, respectively, one 12-24 h before transfection. Cells were transiently transfected with Lipofectamine 2000 (Invitrogen) using 1 μg (24-wellplate)or4 μg (6-well plate) of the indicated cDNAs at a Lipofectamine:DNA ratio of 2:1. TRVb CHO cells[41] lacking endogenous TfR expression and AN27 cells[30,42] were donated by T.E. McGraw (Weill College of Medicine, Cornell University, New York) and K. Prasad (Colorado Health Sciences Center, Denver), respectively, and were maintained as previously described. TRVb CHO cells were plated at 1.25×10^5 cells/well on glass coverslips in 24-well plates 24 h prior to transfection and were transfected with 0.5 μg DNA/well at a lipid:DNA ratio of 3:1, using Lipofectin (Invitrogen) according to the manufacturer's instructions. AN27 cells were plated at 5×10^4 cells/well on glass coverslips in 24-well plates 24 h prior transfection and were transfected with 0.2 μg DNA/well using Effectene (Qiagen) according to the manufacturer's instructions. Cells were routinely assayed 48 h post-transfection.

Primary ventral midbrain neuron cultures and transfections

Postnatal ventral midbrain neurons were isolated from P2 Sprague-Dawley rats and plated on cortical astrocyte monolayers according to previously described methods[43]. All animal procedures were approved by and in accordance with the Institutional Animal Use and Care Committee of the University of Massachusetts Medical School. Briefly, P2 rat pups were killed by ketamine overdose and decapitation, and brains were rapidly removed. Ventral midbrains were dissected, minced and digested with papain (20 units/ml, 1 h, 36 °C, 95% O_2/5% CO_2), pooling 3-4 ventral midbrains per digestion. Tissue chunks were washed in SF1C media and were dissociated by trituration, first through a P1000 tip, and then progressively through 20-, 22- and 25-gauge needles. Dissociated cells were collected by centrifugation (1048*g*, 5 min), resuspended in SF1C, and plated at 1.6×10^5 cells/well on cortical astrocyte monolayers grown on glass coverslips in 24-well tissue culture plates. GDNF (10 ng/ml, Chemicon) was added to the cultures 90 min after plating, and 5-fluro-2′-deoxyuridine (6.7 μg/ml) was added 24 h after plating to inhibit glial proliferation. Neurons were cultured for 21 d after plating to allow for maximal expression of the dopaminergic phenotype, defined as positive immunofluorescent staining for both tyrosine hydroxylase and DAT. Neurons were transfected with Lipofectamine 2000 at a lipid:DNA ratio of 2:1, using 1.0 μg DNA per well. Transfection mixtures were added directly to fresh media in the wells and were incubated with cells until assays were performed 48 h post-transfection.

Uptake assays

Uptake assays were performed as previously described[13]. Briefly, cells were washed repeatedly in Krebs-Ringers-HEPES (KRH) buffer and preincubated in KRH containing 0.18% glucose and either vehicle or 1 μM PMA (30 min, 37 °C). Uptake was initiated by adding 1 μM[^{3}H]DA (3,4-[ring-2,5,6,-^{3}H]DA, Perkin Elmer) containing 10^{-5} M pargyline and 10^{-5} M ascorbic acid. Uptake proceeded for 10 min at 37 °C and was terminated with three rapid washes in ice-cold KRH buffer. Cells were lysed in scintillation fluid and counted in a Microbeta plate counter (Wallac). Nonspecific uptake was defined in the presence of 10 μM GBR12909, and all samples included 100 nM desipramine to block uptake contribution by endogenously expressed NET.

Cell-surface biotinylation

Cell-surface proteins were biotinylated with the membrane-impermeant reagent NHS-SS-biotin (1.0 mg/ml) in phosphate buffered saline (PBS) containing 1.0 mM $MgCl_2$, 0.1 mM $CaCl_2$ (PBS^{2+}) as described previously[13,15]. Cells were subsequently washed in PBS^{2+}, lysed (20 min, 4 °C) in RIPA buffer (10 mM Tris, pH 7.4, 150 mM NaCl, 1.0 mM EDTA, 0.1% SDS, 1.0% Triton X-100, and 1.0% sodium deoxycholate) containing protease inhibitors (1.0 mM PMSF, 1.0 μg/ml leupeptin, 1.0 μg/ml pepstatin and 1.0 μg/ml aprotinin); lysates were cleared by centrifugation. Protein concentrations were determined using the BCA protein assay kit (Pierce), and biotinylated and non-biotinylated proteins from equivalent amounts of total cellular protein were separated by streptavidin-agarose affinity chromatography. Samples were analyzed by SDS-PAGE and immunoblot, and DAT-positive bands were detected with SuperSignal West Dura Extended substrate (Pierce). Nonsaturating, immunoreactive bands were captured using a CCD camera gel documentation system and were quantitated using Quantity One software (Bio-Rad).

Transporter internalization assay

Relative transporter internalization rates were measured as previously described[15]. Briefly, transiently transfected PC12 cells, plated in 6-well plates, were labeled with 2.5 mg/ml sulfo-NHS-SS-biotin. After glycine quenching, zero time points (total surface pools and strip controls) were left at 4 °C, and internalization samples were warmed to 37 °C by multiple rapid washes in prewarmed PBS^{2+}, 0.18% glucose, 0.2% IgG/protease-free bovine serum albumin (BSA; PBS^{2+}/g/BSA) and were incubated in the same solution (10 min, 37 °C). Internalization was stopped by washing repeatedly in ice-cold NT Buffer, and residual surface biotin was stripped from internalization samples and strip controls by reducing in 100 mM mercaptoethanesulfonic acid (NT buffer, washed twice, 25 min each time, 4 °C). Cells were washed repeatedly in NT buffer and PBS^{2+}, and were lysed in RIPA; biotinylated proteins were isolated and analyzed as described above. Strip efficiencies were calculated for each sample and were typically >90% of total labeled protein at the zero timepoint.

Transferrin uptake

Transfected TRVb cells were washed with PBS and serum starved in OPTIMEM (30 min, 37 °C, 5% CO_2), followed by incubation in Tf-Alexa594 (60 μg/μl, 30 min, 4 °C) to label surface TfR. Internalization was initiated by rapidly warming cells for the times indicated and was stopped by washing repeatedly with ice-cold PBS. Cells were fixed in 4% paraformaldehyde and washed with PBS, and coverslips were dried and mounted in Prolong Gold Mounting media (Molecular Probes). Cells were imaged with wide-field microscopy, as described below.

Tac internalization assays

Transiently transfected PC12 and AN27 cells, plated on glass coverslips, were washed with ice cold PBS and were labeled (0.4 μg/ml, 1 h, 4 °C) with mouse anti-Tac antibody (Upstate)

in PBS^{2+}/g/BSA. For primary ventral midbrain neurons, cells were kept at 37 °C in their culture medium, and antibody to Tac (anti-Tac) was added at a final concentration of 0.4 μg/ml. Internalization was initiated by shifting cells to 37 °C and proceeded for 20 min. Cells were washed in PBS, fixed in 4% paraformaldehyde and permeabilized with 0.2% Triton X-100; internalized anti-Tac was detected with Alexa594-conjugated anti-mouse secondary antibody (1:5,000, 45 min, 23 °C). Cells were washed and coverslips were dried, mounted and assessed with widefield microscopy as described below. Positive internalization was scored only in cases where all surface staining was lost, as compared with Tac negative controls, with a parallel appearance of intracellular puncta. Puncta intracellular localization was confirmed by co-localization with internalized transferrin.

Wide-field microscopy and image analysis

Cells were visualized with a Zeiss Axiovert 200M microscope using a 63×, 1.4 N.A. oil-immersion objective, and 0.4-μm optical sections were captured through the z-axis with a Retiga-1300R cooled CCD camera (Qimaging) using Slidebook 4.0 software (Intelligent Imaging Innovations). *Z*-stacks were deconvolved with a constrained iterative algorithm using measured point spread functions for each fluorescent channel using Slidebook 4.0 software. All images shown are single 0.4-μm planes through the center of each cell.

ACKNOWLEDGMENTS

We thank Z. Stevens for excellent technical assistance and D. LaPointe for bioinformatics support. We are grateful to V. Budnik, P. Gardner and D. Lambright for critical manuscript review and helpful discussions. This work was supported by National Institute on Drug Abuse award 15169 to H.E.M.

References

1. Chen NH, Reith ME, Quick MW. Synaptic uptake and beyond: the sodium- and chloride-dependent neurotransmitter transporter family SLC6. Pflugers Arch 2004;447:519–531. [PubMed: 12719981]
2. Torres GE, Gainetdinov RR, Caron MG. Plasma membrane monoamine transporters: structure, regulation and function. Nat. Rev. Neurosci 2003;4:13–25. [PubMed: 12511858]
3. Rothman RB, Baumann MH. Monoamine transporters and psychostimulant drugs. Eur. J. Pharmacol 2003;479:23–40. [PubMed: 14612135]
4. Schenk JO. The functioning neuronal transporter for dopamine: kinetic mechanisms and effects of amphetamines, cocaine and methylphenidate. Prog. Drug Res 2002;59:111–131. [PubMed: 12458965]
5. Gulley JM, Zahniser NR. Rapid regulation of dopamine transporter function by substrates blockers and presynaptic receptor ligands. Eur. J. Pharmacol 2003;479:139–152. [PubMed: 14612145]
6. Amara SG, Sonders MS. Neurotransmitter transporters as molecular targets for addictive drugs. Drug Alcohol Depend 1998;51:87–96. [PubMed: 9716932]
7. Jones SR, et al. Profound neuronal plasticity in response to inactivation of the dopamine transporter. Proc. Natl. Acad. Sci. USA 1998;95:4029–4034. [PubMed: 9520487]
8. Zhuang X, et al. Hyperactivity and impaired response habituation in hyperdopaminergic mice. Proc. Natl. Acad. Sci. USA 2001;98:1982–1987. [PubMed: 11172062]
9. Melikian HE. Neurotransmitter transporter trafficking: endocytosis, recycling and regulation. Pharmacol. Ther 2004;104:17–27. [PubMed: 15500906]
10. Zahniser NR, Doolen S. Chronic and acute regulation of Na+/Cl-dependent neurotransmitter transporters: drugs, substrates, presynaptic receptors, and signaling systems. Pharmacol. Ther 2001;92:21–55. [PubMed: 11750035]
11. Robinson MB. Regulated trafficking of neurotransmitter transporters: common notes but different melodies. J. Neurochem 2002;80:1–11. [PubMed: 11796738]
12. Daniels GM, Amara SG. Regulated trafficking of the human dopamine transporter. Clathrin-mediated internalization and lysosomal degradation in response to phorbol esters. J. Biol. Chem 1999;274:35794–35801. [PubMed: 10585462]

13. Melikian HE, Buckley KM. Membrane trafficking regulates the activity of the human dopamine transporter. J. Neurosci 1999;19:7699–7710. [PubMed: 10479674]
14. Li LB, et al. The role of *N*-glycosylation in function and surface trafficking of the human dopamine transporter. J. Biol. Chem. 2004
15. Loder MK, Melikian HE. The dopamine transporter constitutively internalizes and recycles in a protein kinase C-regulated manner in stably transfected PC12 cell lines. J. Biol. Chem 2003;278:22168–22174. [PubMed: 12682063]
16. Deken SL, Wang D, Quick MW. Plasma membrane GABA transporters reside on distinct vesicles and undergo rapid regulated recycling. J. Neurosci 2003;23:1563–1568. [PubMed: 12629157]
17. Whitworth TL, Quick MW. Substrate-induced regulation of γ-aminobutyric acid transporter trafficking requires tyrosine phosphorylation. J. Biol. Chem 2001;276:42932–42937. [PubMed: 11555659]
18. Whitworth TL, Herndon LC, Quick MW. Psychostimulants differentially regulate serotonin transporter expression in thalamocortical neurons. J. Neurosci 2002;22:RC192. [PubMed: 11756522]
19. Zhu CB, Hewlett WA, Feoktistov I, Biaggioni I, Blakely RD. Adenosine receptor, protein kinase G, and p38 mitogen-activated protein kinase-dependent up-regulation of serotonin transporters involves both transporter trafficking and activation. Mol. Pharmacol 2004;65:1462–1474. [PubMed: 15155839]
20. Law RM, Stafford A, Quick MW. Functional regulation of γ-aminobutyric acid transporters by direct tyrosine phosphorylation. J. Biol. Chem 2000;275:23986–23991. [PubMed: 10816599]
21. Quick MW, Hu J, Wang D, Zhang HY. Regulation of a γ-aminobutyric acid transporter by reciprocal tyrosine and serine phosphorylation. J. Biol. Chem 2004;279:15961–15967. [PubMed: 14761965]
22. Bonifacino JS, Traub LM. Signals for sorting of transmembrane proteins to endosomes and lysosomes. Annu. Rev. Biochem 2003;72:395–447. [PubMed: 12651740]
23. Dell'Angelica EC. Clathrin-binding proteins: got a motif? Join the network! Trends Cell Biol 2001;11:315–318. [PubMed: 11489622]
24. Subtil A, Lampson MA, Keller SR, McGraw TE. Characterization of the insulin-regulated endocytic recycling mechanism in 3t3-l1 adipocytes using a novel reporter molecule. J. Biol. Chem 2000;275:4787–4795. [PubMed: 10671512]
25. Johnson AO, Lampson MA, McGraw TEA. Di-leucine sequence and a cluster of acidic amino acids are required for dynamic retention in the endosomal recycling compartment of fibroblasts. Mol. Biol. Cell 2001;12:367–381. [PubMed: 11179421]
26. Tan PK, Waites C, Liu Y, Krantz DE, Edwards RHA. Leucine-based motif mediates the endocytosis of vesicular monoamine and acetylcholine transporters. J. Biol. Chem 1998;273:17351–17360. [PubMed: 9651318]
27. Aguilar RC, et al. Signal-binding specificity of the μ4 subunit of the adaptor protein complex AP-4. J. Biol. Chem 2001;276:13145–13152. [PubMed: 11139587]
28. Madsen KL, et al. Molecular determinants for the complex binding specificity of the PDZ domain in PICK 1. J. Biol. Chem. published online 17 March 2005 (doi:10.1074/ jbc.M500577200)
29. Bjerggaard C, et al. Surface targeting of the dopamine transporter involves discrete epitopes in the distal C terminus but does not require canonical PDZ domain interactions. J. Neurosci 2004;24:7024–7036. [PubMed: 15295038]
30. Torres GE, et al. Functional interaction between monoamine plasma membrane transporters and the synaptic PDZ domain-containing protein PICK1. Neuron 2001;30:121–134. [PubMed: 11343649]
31. Loland CJ, Norregaard L, Litman T, Gether U. Generation of an activating Zn^{2+}switch in the dopamine transporter: mutation of an intracellular tyrosine constitutively alters the conformational equilibrium of the transport cycle. Proc. Natl. Acad. Sci. USA 2002;99:1683–1688. [PubMed: 11818545]
32. Saunders C, et al. Amphetamine-induced loss of human dopamine transporter activity: an internalization-dependent and cocaine-sensitive mechanism. Proc. Natl. Acad. Sci. USA 2000;97:6850–6855. [PubMed: 10823899]
33. Moron JA, et al. Mitogen-activated protein kinase regulates dopamine transporter surface expression and dopamine transport capacity. J. Neurosci 2003;23:8480–8488. [PubMed: 13679416]

34. Jayanthi LD, Samuvel DJ, Ramamoorthy S. Regulated internalization and phosphorylation of the native norepinephrine transporter in response to phorbol esters: evidence for localization in lipid rafts and lipid raft-mediated internalization. J. Biol. Chem 2004;279:19315–19326. [PubMed: 14976208]

35. Farhan H, et al. Two discontinuous segments in the carboxy terminus are required for membrane targeting of the rat GABA transporter-1 (GAT1). J. Biol. Chem 2004;279:28553–28563. [PubMed: 15073174]

36. Sorkin A, Von Zastrow M. Signal transduction and endocytosis: close encounters of many kinds. Nat. Rev. Mol. Cell Biol 2002;3:600–614. [PubMed: 12154371]

37. Ginty DD, Segal RA. Retrograde neurotrophin signaling: Trk-ing along the axon. Curr. Opin. Neurobiol 2002;12:268–274. [PubMed: 12049932]

38. Bredt DS, Nicoll RA. AMPA receptor trafficking at excitatory synapses. Neuron 2003;40:361–379. [PubMed: 14556714]

39. Malinow R, Malenka RC. AMPA receptor trafficking and synaptic plasticity. Annu. Rev. Neurosci 2002;25:103–126. [PubMed: 12052905]

40. Ali SA, Steinkasserer A. PCR-ligation-PCR mutagenesis: a protocol for creating gene fusions and mutations. Biotechniques 1995;18:746–750. [PubMed: 7619468]

41. Johnson AO, et al. Transferrin receptor containing the SDYQRL motif of TGN38 causes a reorganization of the recycling compartment but is not targeted to the TGN. J. Cell Biol 1996;135:1749–1762. [PubMed: 8991088]

42. La Rosa FG, et al. Inhibition of proliferation and expression of T-antigen in SV40 large T-antigen gene-induced immortalized cells following transplantations. Cancer Lett 1997;113:55–60. [PubMed: 9065801]

43. Mena MA, Davila V, Sulzer D. Neurotrophic effects of L-DOPA in postnatal midbrain dopamine neuron/cortical astrocyte cocultures. J. Neurochem 1997;69:1398–1408. [PubMed: 9326268]

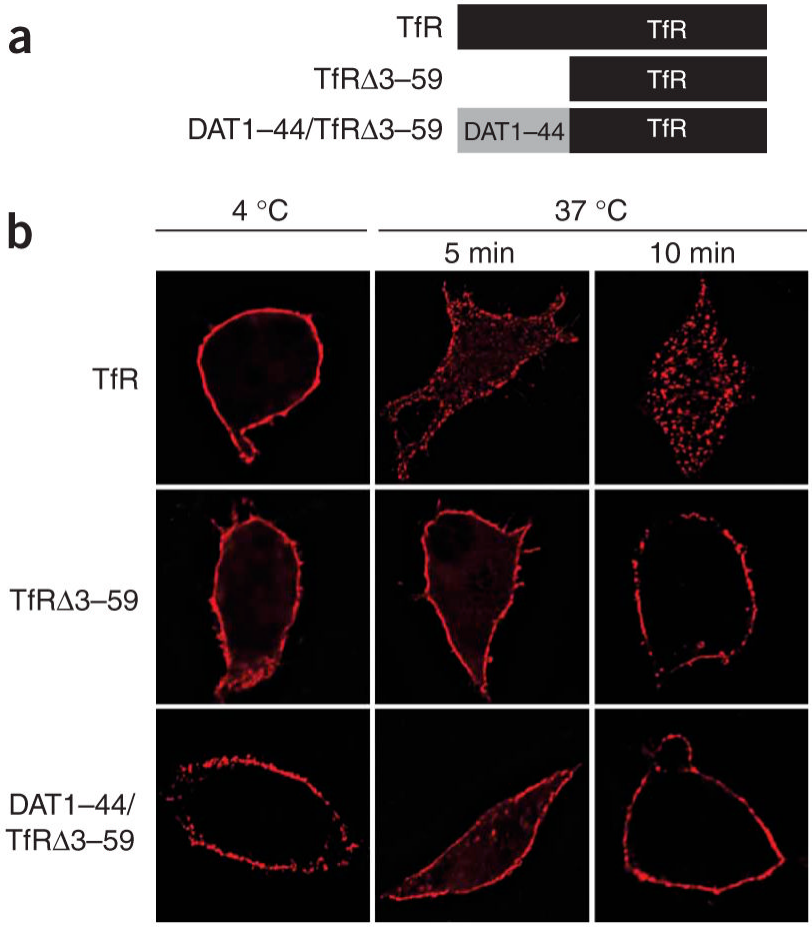

Figure 1.

The DAT N terminus does not contain an autonomous endocytic signal. (**a**) Schematic representation of wild-type, Δ3-59 truncated (endocytic-deficient) and DAT-chimeric TfR. (**b**) Transferrin internalization assay. Tf-Alexa594 was applied to serum-starved, transfected TRVb cells for the times indicated, and cells were fixed, mounted and imaged by wide-field microscopy. Note loss of surface staining and appearance of intracellular puncta for wild-type TfR, indicative of internalization. Representative cells are shown, $n = 2$.

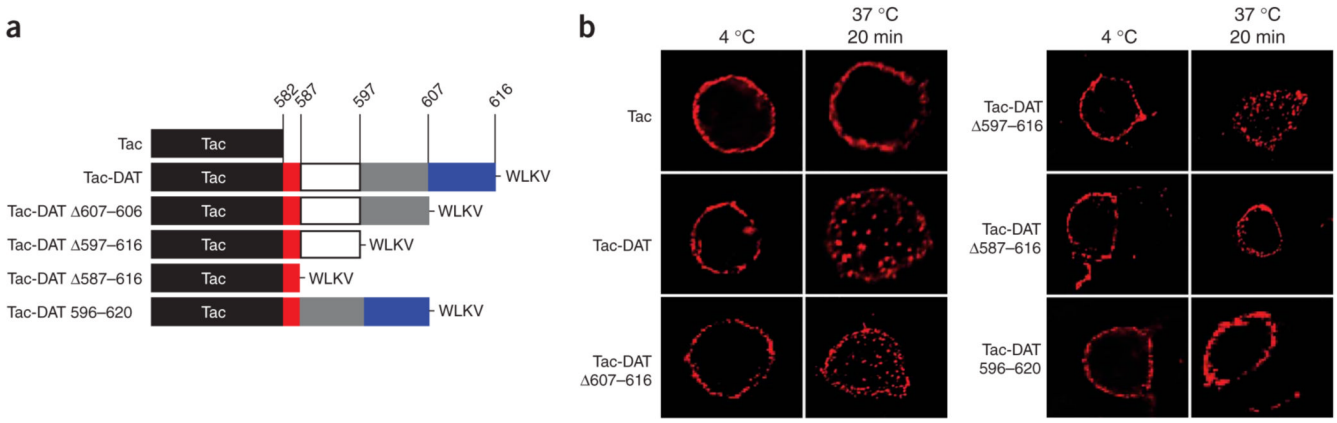

Figure 2.

DAT C-terminal residues 587-596 are sufficient to drive Tac endocytosis. (**a**) Schematic representation of the interleukin-2α receptor (Tac) and chimeric Tac-DAT proteins. (**b**) Single-cell Tac internalization assay. Antibody to Tac (anti-Tac) was bound at 4 °C to cells transfected with the indicated Tac-DAT cDNAs, and cells were warmed to 37 °C for 20 min. Internalized anti-Tac was detected with fluorescently labeled secondary antibodies using wide-field microscopy and image deconvolution. Internalization was scored in cases where Tac surface staining was lost, with a parallel appearance of intracellular puncta. Representative cells are shown. See Table 1 for summary of results.

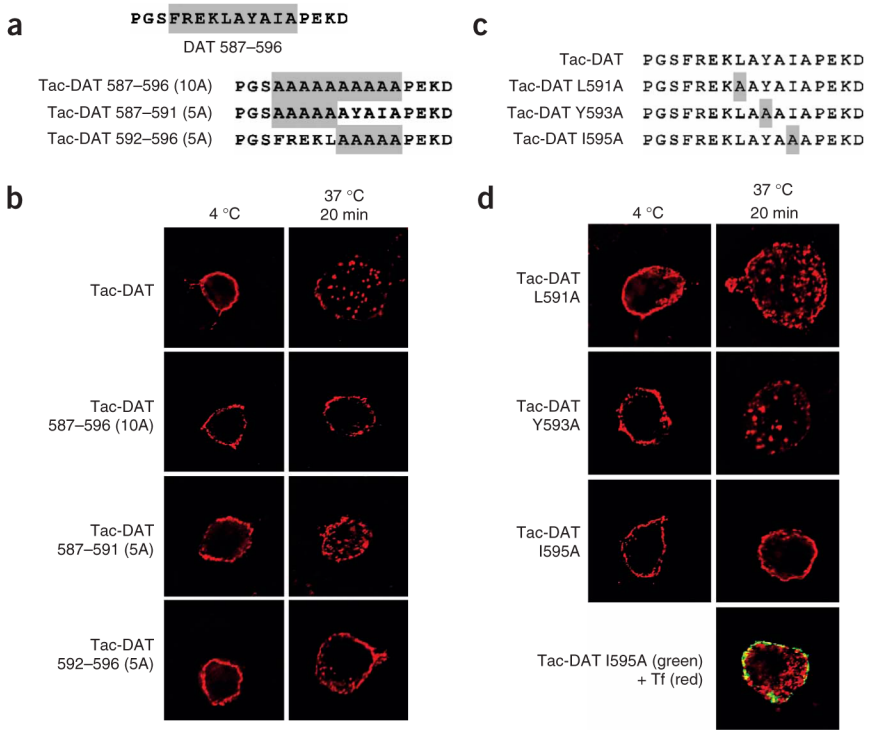

Figure 3.

DAT Ile595 within the FREKLAYAIA sequence is necessary for Tac-DAT endocytosis. (**a,c**) DAT sequence illustrating the FREKLAYAIA sequence spanning DAT residues 587-596. Residues targeted for mutagenesis are shaded. (**b,d**) Single-cell Tac internalization assay. Internalization was scored in cases where Tac surface staining was lost, with a parallel appearance of intracellular puncta (see Methods). Global endocytosis in cells expressing Tac-DAT I595A (**d**, green) was validated by transferrin uptake with Tf-Alexa594 (red). Representative cells are shown for each condition. See Table 1 for summary of results.

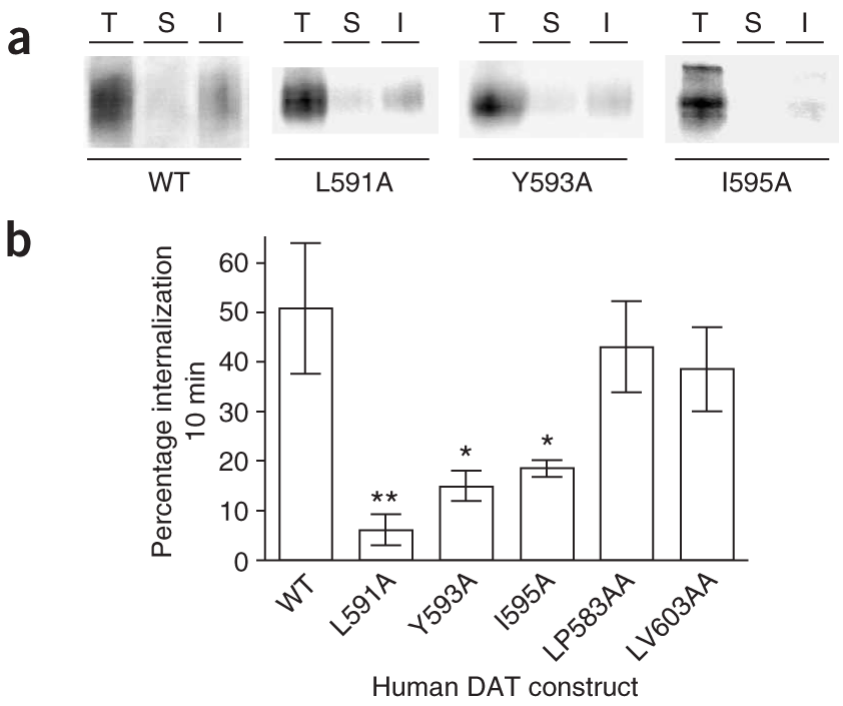

Figure 4.

Nonpolar residues within the FREKLAYAIA sequence are necessary for constitutive DAT internalization as shown by DAT internalization assay. Cells transfected with the indicated DAT cDNAs were surface biotinylated, and the percentage total DAT internalizing in 10 min was measured (see Methods). (**a**) Representative DAT immunoblots detecting total initial DAT surface pools (T), strip controls (S) and internalized DAT (I) for wild-type DAT (WT) and the indicated DAT mutants. (**b**) Average internalization data. Bars represent the percentage DAT internalized over 10 min at 37 °C, compared with total surface DAT at time zero, ±s.e.m. **P* < 0.05, ***P* < 0.01, one-way ANOVA with Dunnett's multiple comparison test; *n* = 2-5.

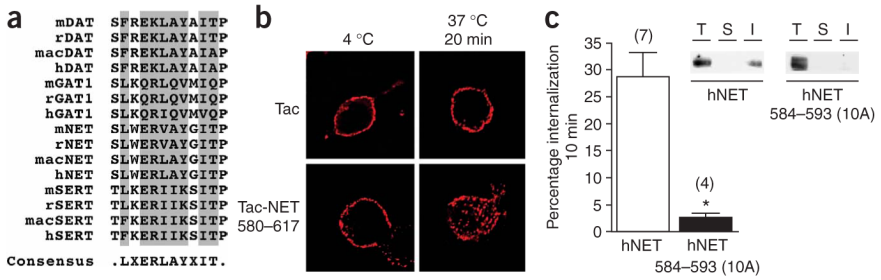

Figure 5.

The FREKLAYAIA region is conserved in SLC6 neurotransmitter transporters and is both necessary and sufficient for NET endocytosis. (**a**) Amino acid sequence alignment of the DAT FREKLAYAIA region and the orthologous domain in rodent (mouse (m) and rat (r)) and primate (macaque (mac) and human (h)) SLC6 neurotransmitter transporters, with conserved residues shaded. The consensus sequence is indicated below the alignment. SERT, serotonin transporter. (**b**) Tac internalization assay. Tac and Tac-NET(580-617) were expressed in PC12 cells and their endocytic potential was assessed by antibody uptake with anti-Tac (see Methods). Representative cells are shown; $n = 5$. (**c**) NET internalization assay. Cells were transiently transfected with wild-type hNET or hNET584-593(10A) cDNAs, and internalization was measured as described in Methods.Bars represent the percentage NET internalized over 10 min at 37 °C compared with total surface NET at time zero, ±s.e.m; *n* values are indicated above the bars, $*P < 0.002$, Student's *t*-test. Inset: representative immunoblot detecting total initial NET surface pools (T), strip controls (S) and internalized NET (I) for wild-type hNET and hNET584-593(10A).

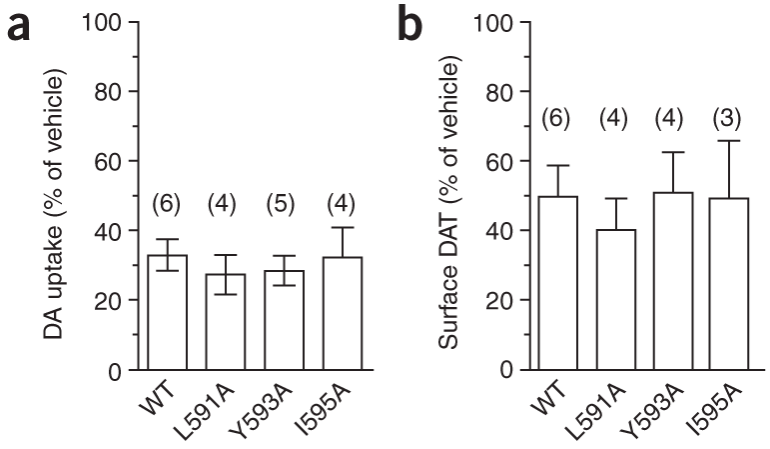

Figure 6.

Nonpolar residues within the FREKLAYAIA sequence are not required for PKC-stimulated DAT downregulation and internalization. (**a**) DA uptake assay of transfected PC12 cells preincubated with vehicle or 1 μM PMA, 30 min. Data are expressed as percentage uptake compared with vehicle-treated cells, ±s.e.m. (**b**) Cell-surface biotinylation of transfected PC12 cells following 30-min treatment with either vehicle or 1 μM PMA. Bar graph of averaged data expressed as percentage biotinylated DAT as compared with vehicle-treated cells, ±s.e.m. **P* < 0.01, one-way ANOVA with Bonnferoni multiple comparison test; *n* values indicated above each bar.

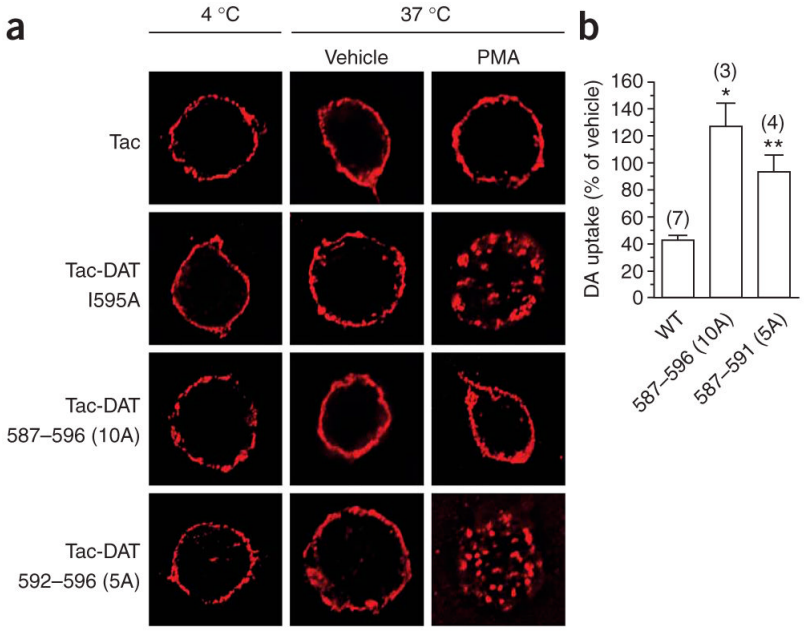

Figure 7.

The DAT C terminus contains a PKC-sensitive endocytic signal. (**a**) Tac internalization assay. PC12 cells transfected with the indicated Tac proteins incubated with anti-Tac at either 4 °C or 37 °C in the presence of either vehicle or 1 μM PMA. Images are representative of 3-4 cells imaged per experiment; $n = 4$. (**b**) DA uptake assay. Cells transfected with wild-type DAT (WT) or the indicated DAT mutants were treated with either vehicle or 1 μM PMA for 30 min at 37 °C, and DA uptake was assessed as described in Methods. Bars indicate percentage DA uptake as compared with vehicle-treated cells ± s.e.m. Asterisks indicate values significantly different from wild type, $*P < 0.001$, $**P < 0.01$, one-way ANOVA with Bonferroni multiple comparisons test; *n* values are indicated above the bars.

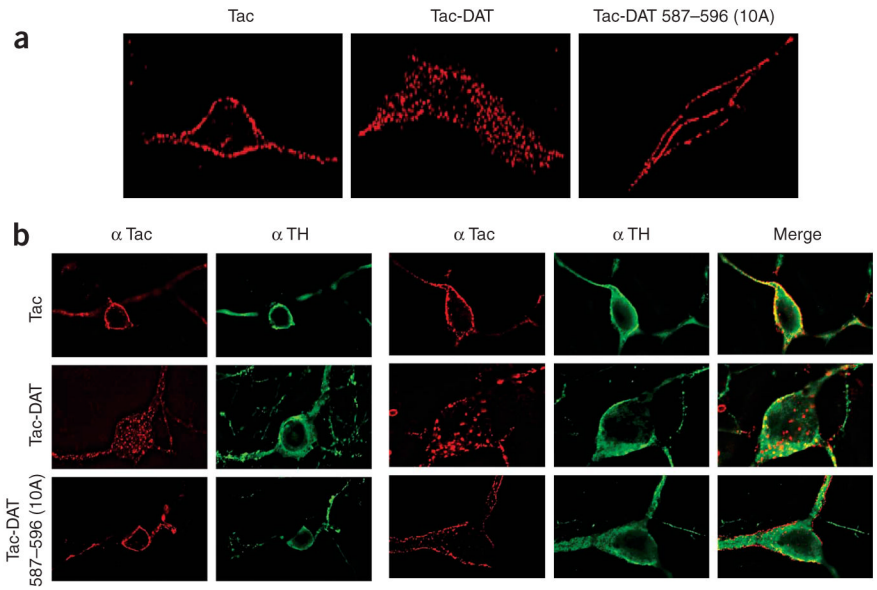

Figure 8.

DAT C-terminal residues 587-596 are sufficient and necessary to drive endocytosis in dopaminergic cells. Immortalized mesencephalic AN27 cells (**a**) and primary ventral midbrain neurons (**b**) were transfected with the indicated Tac proteins and anti-Tac internalization was assessed. Representative images are shown. For AN27 cells, 7-10 cells were imaged per Tac construct, $n = 2$; for primary ventral midbrain neurons, 11-16 cells were imaged per Tac construct, $n = 3$-5.

Table 1

Single-cell Tac internalization assay

Tac construct	*n*	Total number of cells imaged	Percentage of cells showing internalization
Tac	26	77	2.3 ± 1.6
Tac-DAT 582-620*	21	81	93.0 ± 2.7
Tac-DAT 596-620	7	27	18.3 ± 7.4
Tac-DAT Δ607-616*	2	6	100.0 ± 0.0
Tac-DAT Δ596-616*	2	4	100.0 ± 0.0
Tac-DAT Δ587-616*	2	6	12.5 ± 12.5
Tac-DAT 587-596(10A)	8	30	17.1 ± 7.1
Tac-DAT 587-591(5A)*	6	28	60.0 ± 11.0
Tac-DAT 592-596(5A)	5	16	15.0 ± 10.0
Tac-DAT L591A*	3	17	83.3 ± 8.3
Tac-DAT Y593A*	3	18	90.0 ± 9.1
Tac-DAT I595A	10	43	12.4 ± 4.2

*Significantly different from Tac, $P < 0.01$, one-way ANOVA with Dunnett's multiple comparison test.